J. Membrane Biol. 73, 95–102 (1983)

The Journal of
Membrane Biology

Ionic Selectivity of the Paracellular Shunt Path across Rabbit Corneal Endothelium

Jong J. Lim[+], Larry S. Liebovitch[+] and Jorge Fischbarg[+*]
Departments of Opthalmology[+] and Physiology,[*+]
College of Physicians and Surgeons, Columbia University, New York, New York 10032

Summary. We have measured the dilution and biionic potentials across the isolated rabbit corneal endothelium in order to learn about the ionic selectivity of its intercellular junctions. Single-salt dilution potentials have been measured as a function of [NaCl] or [$NaHCO_3$] gradients across the tissue. Biionic potentials were similarly measured by replacing Na^+ with K^+ on either side of the tissue. The potentials thus measured were fit to the constant field equation and to an approximation of it to obtain the ionic permeabilities for K^+, HCO_3^- and Cl^- relative to Na^+. The permeability sequence obtained was $P_K > P_{Na} > P_{HCO_3} \cong P_{Cl}$. Potentials were also measured after imposing an osmotic gradient across the preparation using sucrose. The results obtained with all these methods are consistent and suggest that this tissue is slightly more permeant to cations than anions, but that the selectivity of the intercellular junction is relatively low. From these experiments, a 30 mM gradient of salt across the endothelial layer would be needed in order to explain the observed spontaneous potential difference (about 1 mV, aqueous negative) across that layer if the potential was due to the selectivity of the intercellular junctions. Such a value for the gradient is much larger than theoretical estimates of it; therefore, we favor electrogenic transport of HCO_3^- as a better explanation for the origin of the spontaneous potential difference.

Key Words dilution potential · biionic potential · permeability ratios · constant field equation · electrogenic transport · rabbit corneal endothelium

Introduction

In recent years, intensive efforts have been devoted to the study of the physiological basis for the maintenance of corneal transparency. It is generally accepted (*cf.* Maurice, 1969) that such transparency is maintained by the limiting cell layers of the cornea. The corneal stroma has a normal tendency to swell and become opaque because it contains water-avid mucopolysaccharides. Hence, in order to maintain constant stromal thickness, the fluid that leaks into the stroma must be pumped out. The endothelium performs just that function, transporting fluid from the stroma towards the aqueous at a rate of about 5 $\mu l/hr \cdot cm^2$ (Maurice, 1972; Fischbarg, Lim & Bourguet, 1977). The epithelium, in turn, acts as a barrier but appears to transport relatively little fluid across it (Klyce, 1977), at least in mammals such as the rabbit.

For the case of the endothelium, the electrical characteristics of the tissue have been measured (Fischbarg, 1972, 1973; Fischbarg & Lim, 1973, 1974; Barfort & Maurice, 1974; Hodson, 1974; Lim & Fichbarg, 1981) as have the intracellular potentials (Wiederholt & Koch, 1978; Lim & Fischbarg, 1979). From these reports, it is evident that there is a small potential difference across the endothelial preparation (about 1 mV, aqueous side negative); that is consistent with the small transendothelial electrical resistance of about 30 to 70 $\Omega\,cm^2$ which shunts the transcellular pathway. The magnitude of the intracellular potentials is comparable to that reported for other transporting epithelia.

The basis for the transendothelial potential difference is still unclear, however, Thus far, it has been reported that, as in other epithelia, the transendothelial potential difference and fluid transport are critically dependent on the presence of sodium ions in solution (Fischbarg & Lim, 1974; Hodson, 1974). A net flux of Na^+ across the endothelium has been found recently by conventional flux measurements (Huff & Green, 1981; Lim, 1981*a*, *b*; Lim & Ussing, 1982). However, since the transendothelial potential difference is oriented with the aqueous side negative and the direction of the net Na^+ movement is from stroma to aqueous (just as that of fluid transport), one cannot explain the polarity of the transendothelial potential simply in terms of the net Na^+ movement.

The potential difference might, instead, originate from the transport of an anion towards the aqueous and/or a cation towards the stroma (*cf.* Fischbarg & Lim, 1974; Hodson, 1974). This is conceivable, in principle, since both the potential difference and the fluid transport are critically dependent on ambient [HCO_3^-] (Dikstein & Maurice,

1972; Fischbarg & Lim, 1974; Hodson, 1974) and since a net transendothelial HCO_3^- flux (from stroma to aqueous) has in fact been measured (Hodson & Miller, 1976; Hull, Green, Boyd & Wynn, 1977). Yet, since both HCO_3^- and Na^+ are translocated across the preparation, the pumping mechanism could also be neutral. In that case, the polarity observed for the potential difference could be accounted for if the $NaHCO_3$ transported would diffuse back towards the stroma across cation-selective intercellular junctions. The present study was undertaken in order to explore precisely the latter possibility.

Materials and Methods

The detailed procedure for dissecting the endothelial preparation and mounting it in an experimental chamber has been previously described (Fischbarg & Lim, 1974; Lim & Fischbarg, 1981). As a rule, after mounting that preparation, the transendothelial electrical potential difference (PD) and resistance were monitored for about one hour. If the magnitude of those parameters was within the normal range (greater than 400 μV), the experiment continued and the planned solution exchanges were performed.

Solutions

The regular solution utilized for the control experiments was as follows (in mM): NaCl, 110.4; $NaHCO_3$, 39.2; $KHCO_3$, 3.8; KH_2PO_4, 1.0; $MgSO_4$, 7; H_2O, 0.78; $CaCl_2$, 1.7; Glucose, 6.9. The pH of the solution was adjusted to 7.4 before the beginning of the experiment by bubbling CO_2 through it. This regular solution corresponds to the BSG solution (basal salt with glucose) given in our previous papers (Fischbarg, Lim & Bourguet, 1977; Lim & Fischbarg, 1981). The chamber temperature was kept at 36.0 °C.

Electrical Measurements

a) Potential Difference (PD). The spontaneously generated transendothelial potential difference was measured by using calomel electrodes joined to the experimental chamber through agar-saline bridges. When the same solutions were present on both sides of the preparation, the small potential differences that arose at the junctions between the solutions and the agar bridges were corrected by placing both bridges on the same hemi-chamber and adjusting a series battery. When the preparation was bathed by different solutions on both sides, the bridge-solution liquid junction PD's were corrected for as follows. For each given concentration difference, the PD arising at the liquid junction between the two solutions in question was measured by immersing bridges filled with isotonic saline in the solutions that were in separate containers while joining the containers with and agar-3 M KCl bridge. The other ends of the saline bridges were connected with the calomel electrodes in a 3-M KCl pool. The PD values thus measured were very close to the values expected from Planck's equation (*cf.* McInnes, 1939). These values were then subtracted from those determined in the experiments in which those same solutions were employed. The electrometer employed (Keithley 610 C) has a resolution of 10 μV.

b) Resistance. These measurements were done by sending pulses of constant current across the preparation. Voltage pulses from a generator (pulse width: 100 msec; interval between pulses: 5 sec) were converted to current pulses by an isolation unit (W.P.I., model P.C. 1). The electrodes used to send the current and to record the voltage induced across the preparation have been detailed in a previous paper (Lim & Fischbarg, 1981). When the pulse was applied, the response reached a steady-state after a very short initial transient.

After the initial PD and the resistance (R_t) were determined, a solution containing less [NaCl] or [$NaHCO_3$] was substituted for the control solution on the aqueous side. Some time (3 to 5 min) was allowed for a new steady state to be reached, after which the PD and the resistance (R_t) were determined once more. The above preparation was then returned to the control ambient condition, and the procedure was repeated for the stromal side. These manipulations could be repeated three or four times during a typical five-hour experiment. For these and other measurements, the deviations reported are standard errors of the mean (SEM).

Dilution Potentials

In order to perform these measurements, the concentrations of NaCl or $NaHCO_3$ were reduced with respect to those in the control medium. When HCO_3^- was replaced, the lowest [HCO_3] was 13.2 mM, at which the pH was adjusted by bubbling the solution with CO_2. These salts were replaced by sucrose on an osmolar basis. The concentrations of the other components were unchanged.

Biionic Potentials

The procedure utilized for these measurements was similar to the one described above for the dilution potential measurements, except that here Na^+ was replaced by K^+ on an osmolar basis.

Data Analysis

The permeability ratio was calculated using both analytical and numerical methods. In principle, one must use the ionic activities rather than their concentrations in order to calculate the permeability ratios from the constant field equation. However, in the range of dilutions presently employed the activity coefficients varied only from 0.72 to 0.80. The replacement of concentrations by activities affects the calculated potential only through such differences in activities between the solutions on both sides of the preparation. For example, in a typical calculation for which concentrations were employed, the permeability ratios (*see below*) were: $\alpha_1 = 1.08$, $\alpha_2 = 0.85$ and $\alpha_3 = 0.82$. When the activities were used instead, the results were: $\alpha_1 = 1.08$, $\alpha_2 = 0.84$ and $\alpha_3 = 0.80$. Since the differences encountered were small, for simplicity, our calculations were done using concentration values.

1a) Fit to the Exact Constant Field Equation (Analytical Method). The constant field equation for two cations and two anions is:

$$\psi_a - \psi_b = (RT/F)\{\log[([Na]_b + \alpha_1[K]_b + \alpha_2[Cl]_a + \alpha_3[HCO_3]_a)/([Na]_a + \alpha_1[K]_a + \alpha_2[Cl]_b + \alpha_3[HCO_3]_b)]\} \quad (1)$$

where the subscripts a and b stand for the aqueous (apical) and stromal (basal) side, respectively, and $\alpha_1 = P_K/P_{Na}$; $\alpha_2 = P_{Cl}/P_{Na}$; $\alpha_3 = P_{HCO_3}/P_{Na}$. In Eq. (1) above there are three unknowns, namely, α_1, α_2 and α_3. Hence, three independent equations are needed in order to be able to solve for the unknowns. These

equations were obtained by substituting into Eq. (1) the PD values measured and the concentration values utilized for the determination of two dilution potentials and one biionic potential. As an example, using the NaCl dilution potential data one gets from Eq. (1) the following:

$$([Na]_b+\alpha_1[K]_b+\alpha_2[Cl]_a+\alpha_3[HCO_3]_a= \{[Na]_a+\alpha_1[K]_a+\alpha_2[Cl]_b+\alpha_3[HCO_3]_b\}e^{F(\psi_a-\psi_b)/RT}. \quad (2)$$

Two additional equations similar to Eq. (2) above are obtained from the $NaHCO_3$ dilution potential, and from the Na^+-K^+ bionic potential. Thus, three data points determine the values of α_1, α_2 and α_3. All the possible combinations of the experimental data points were then used to determine permeability ratios. The median of these values was chosen as the best estimator of α_1, α_2 and α_3.

1b) Fit to the Exact Constant Field Equation (Numerical, Nonlinear Least Squares). The dilution and biionic potentials experimentally measured were fit by a computer to the constant field equation (Goldman, 1943; Hodgkin & Katz, 1949) (*see* Eq. (1) above). The calculations were done with a PDP 11/34 minicomputer (Digital). The subroutines used to perform the nonlinear fit were the ZXSSQ (International Mathematical and Statistical Libraries, Houston, Texas) and the VA05A (Harwell Subroutine Library, Atomic Energy Establishment, Harwell, Berkshire) which minimize the sum of the squares of the differences between theoretically predicted and experimental points. Both subroutines yielded similar results; for convenience we have adopted the ZXSSQ for the present calculation.

2) Fit to a Linear Approximation of the Constant Field Equation. This alternative is based upon an analytical approximation for the solution of the constant field equation. This method will be illustrated by an example constructed with a set of NaCl dilution potential measurements. The concentrations (in mM) of the principal salts in this case were as follows:

Control Solution		*Dilute Solution*	
$[Na]_b$	=150	$[Na]_a$	=60
$[K]_b$	= 3.8	$[K]_a$	= 3.8
$[Cl]_b$	=110	$[Cl]_a$	=20
$[HCO_3]_b$	= 43	$[HCO_3]_a$	=43

The relationships between the Na and the Cl concentrations in the apical and basal sides can be written as:

$$[Na]_a=[Na]_b-x$$
and
$$[Cl]_a=[Cl]_b-x$$

where x represents the concentration difference between the stromal and the aqueous side. Equation (1) above can hence be written as:

$$\psi_a-\psi_b=(RT/F)\log\{A-\alpha_2 x)/(A-x)\},$$
where
$$A=[Na]_b+\alpha_1[K]_b+\alpha_2[Cl]_b+\alpha_3[HCO_3]_b.$$

It follows that:

$$\Delta\psi=(RT/F)\log\{(1-\alpha_2 x/A)/(1-x/A)\}$$
$$=(RT/F)\{\log(1-\alpha_2 x/A)-\log(1-x/A)\}.$$

If one now assumes that $\alpha_2\cong 1$ and $x<A$, the logarithmic expressions are replaced by a linear approximation and one has:

$$\Delta\psi=(RT/F)\{1-\alpha_2\}x/A.$$

Therefore, the slope S_1 is

$$S_1=(RT/F)\{1-\alpha_2\}/A. \quad (4)$$

And similarly for $NaHCO_3$ dilution potentials, and K^+-Na^+ biionic potential measurements, we have

$$S_2=(RT/F)\{1-\alpha_3\}/A \quad (5)$$

$$S_3=(RT/F)\{1-\alpha_1\}/A. \quad (6)$$

From these three equations, one can obtain the three unknows α_1, α_2 and α_3 by using Kramer's rule. The slopes were obtained by eye.

Results

The average transendothelial PD under control conditions was 0.51 ± 0.02 mV (aqueous negative; $n=84$) and the corresponding R_t was 32 ± 1 Ω cm^2 ($n=60$). These values remained reasonably stable for the five hours that a typical experiment required. The dilution and biionic potentials were obtained by subtracting the transendothelial PD above from the potentials induced experimentally.

NaCl Dilution Potentials

A summary of the potentials generated by diluting the NaCl concentration on either side of the preparation is given in Fig. 1. The abscissa represents the NaCl concentration difference (x in Eq. 3) between the solutions on the stromal and aqueous sides. For the positive values, the NaCl concentration was greater on the stromal than on the aqueous side, and vice-versa for negative values. As can be seen in Fig. 1, the data fall on a straight line for the range between -60 and $+90$ mM of

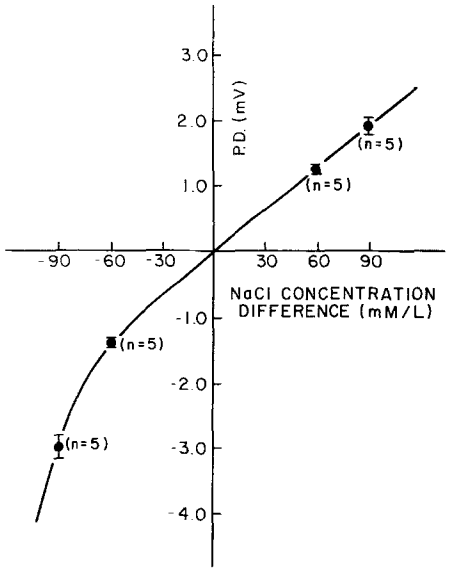

Fig. 1. NaCl dilution potential difference as a function of the salt gradient across the corneal endothelium. The positive abscissa represents the condition in which the solution on the aqueous side has less NaCl than the solution in the stromal side

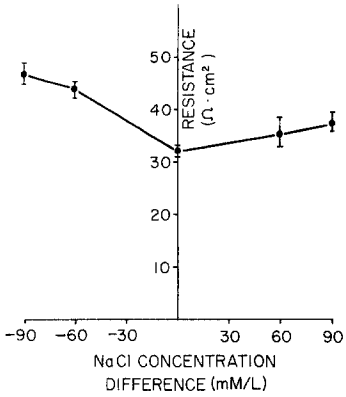

Fig. 2. Transendothelial resistance as a function of NaCl concentration gradient across the preparation. Abscissa as that in Fig. 1

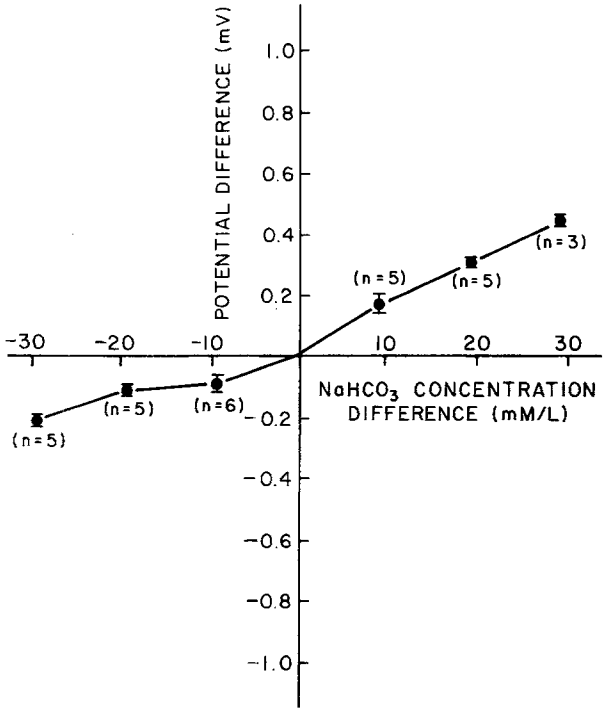

Fig. 3. Same as Fig. 1 except that the gradient arises from a [$NaHCO_3$] difference

the salt gradient. The R_t as a function of the NaCl concentration gradient is shown in Fig. 2. The values of the resistance in the first quadrant do not change significantly with respect to the control condition, whereas the values in the second quadrant increase by some 50% between 0 and −90 mM.

$NaHCO_3$ Dilution Potentials

The results obtained are shown in Fig. 3. The dilution potentials shown in the first quadrant are

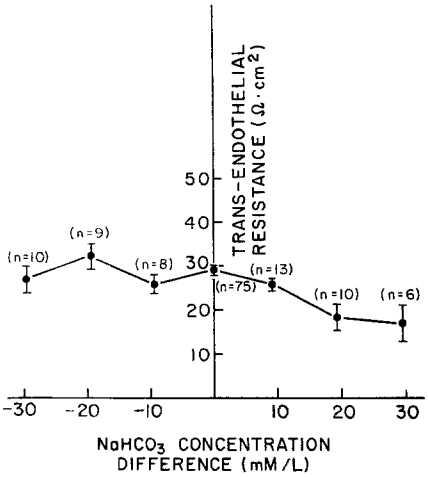

Fig. 4. Transendothelial resistance as a function of [$NaHCO_3$] gradient across the corneal endothelium. Abscissa as that in Fig. 3

linear for the $NaHCO_3$ concentration gradient range tested. The results in the third quadrant are also linear, but the slope is less than that in the first quadrant. The values for R_t as a function of the $NaHCO_3$ concentration gradient are shown in Fig. 4, which shows a slight decrease in the range from 0 to +30 mM of concentration gradient.

K−Na Biionic Potentials

The biionic potentials and the corresponding R_t obtained by replacing Na^+ with K^+ are shown in Figs. 5 and 6, respectively. The positive abscissa represents lower [K^+] on the aqueous side.

Transendothelial Potential Difference and Osmotic Flow

The potential difference resulting from the imposition of a sucrose gradient across the corneal endothelium and the corresponding R_t values are shown in Fig. 7*a* and *b*. Positive and negative values of the abscissa represent sucrose addition to the aqueous and stromal sides, respectively. The transendothelial potential difference (PD) was sensitively dependent on the osmotic gradient imposed. The resistance was more stable: it decreased and increased only by some 20% at large positive and negative gradients, respectively. From the steady-state rate of net fluid movement that corresponds to each value of the osmotic gradient (Fischbarg, Warshavsky & Lim, 1977) and from the PD as a function of the sucrose gradient, one can obtain a plot of the PD versus the rate of the fluid transport shown in Fig. 8*a*. Similarly, the

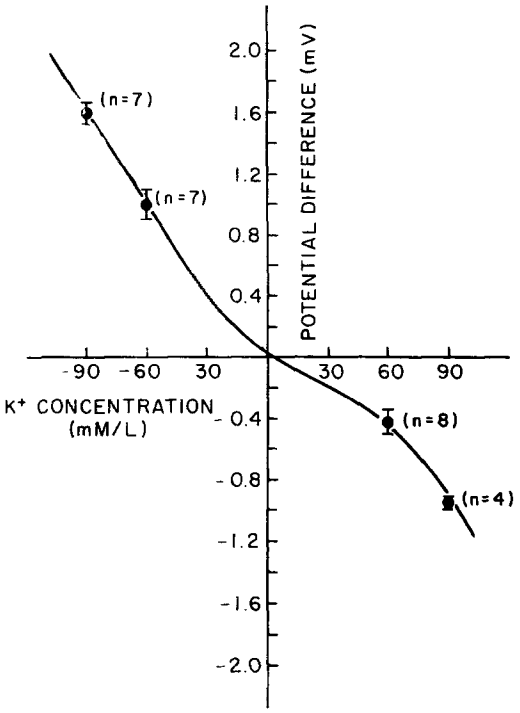

Fig. 5. The Na^+-K^+ biionic potential difference as a function of $[K^+]$. Positive abscissa represents higher $[K^+]$ in the aqueous side than in the stromal side

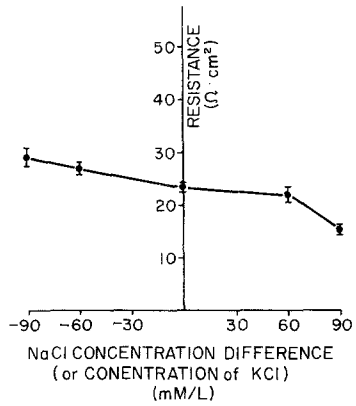

Fig. 6. Transendothelial resistance as a function of $[K^+]$. Abscissa as that in Fig. 5.

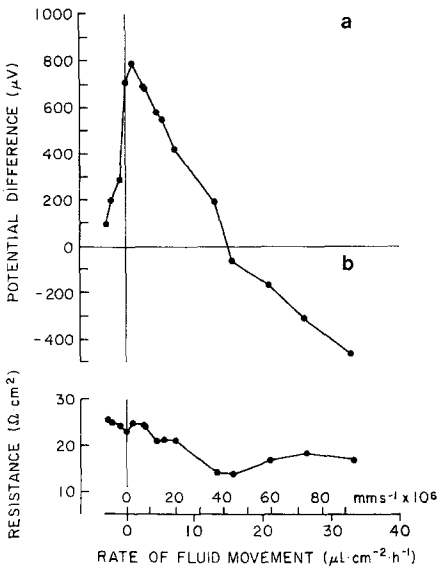

Fig. 7. Potential difference (*a*) and resistance (*b*) with an osmotic (sucrose) gradient across the corneal endothelium. The positive abscissa corresponds to higher osmolarity on the aqueous side

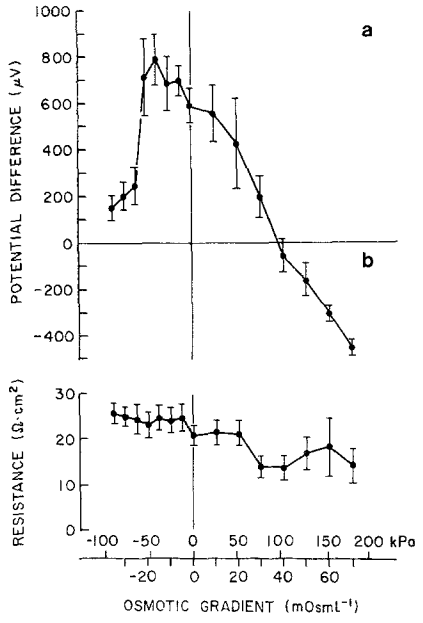

Fig. 8. Transendothelial potential difference (*a*) and resistance (*b*) as a function of the rate of fluid movement generated by an external osmotic (sucrose) gradient

electrical resistance as a function of the rate of fluid transport is shown in Fig. 8*b*.

Permeability Ratios

Table 1 shows a summary of the values determined for the permeability ratios by the different methods utilized here. As can be seen there, the values obtained by the different methods are quite similar. The sequence of the permeabilities is: $P_K > P_{Na} > P_{Cl} \cong P_{HCO_3}$. From the values of the permeability ratios, using a Na^+ permeability value of 0.063 cm/hr obtained from radioisotope-labeled flux measurements (Lim & Ussing, 1982), partial conductances can be calculated for all ions from the equation $g_i = P_i C_i F^2/RT$, where P_i and C_i are the permeability and the concentration of a given ion i and F, R and T are, respectively, Faraday's constant,

Table 1. Permeability ratios obtained from the constant field equation using various methods

	P_K/P_{Na}	P_{Cl}/P_{Na}	P_{HCO_3}/P_{Na}
Fit to the exact constant field equation (analytical)			
Aqueous side hypotonic	1.10±0.01	0.82±0.01	0.79±0.02
Stromal side hyptonic	1.19±0.01	0.78±0.01	0.89±0.01
Fit to the exact constant field equation (numerical, nonlinear least-squares fit)	1.21±0.10	0.90±0.10	0.96±0.10
Fit to a linear approximation of the constant field equation			
Aqueous side hypotonic	1.09	0.76	0.79
Stromal side hypotonic	1.18	0.75	0.94

Deviations are SEM.

Table 2. The measured dilution potentials compared with the potentials calculated using the average permeability ratios determined in this study

	[C]	$(PD)_m$	$(PD)_E$
NaCl Dilution Potentials			
Aqueous	90	1.90	2.10
	60	1.23	1.22
Stromal	90	2.99	2.52
	60	1.42	1.48
$NaHCO_3$ Dilution Potentials			
Aqueous	29.2	0.45	0.62
	19.2	0.31	0.39
	9.2	0.17	0.18
Stromal	29.2	0.21	0.32
	19.2	0.11	0.20
	9.2	0.08	0.09
Biionic Potential (NaCl replaced by KCl)			
Aqueous	90	−0.94	−0.80
	60	−1.00	−1.01
Stromal	90	−1.59	−1.50
	60	−1.00	−1.01

The left column represents the side on which the concentration is manipulated. For detail, *see* Fig. 1 and its legend.
[C] = concentration gradient (in mM/l).
$(PD)_m$ = potential measured (in mV).
$(PD)_E$ = potential calculated by using the constant field equation.

the gas constant and the absolute temperature. The conductances thus obtained are as follows (in mS/cm^2): $g_{Na}=9.11$, $g_K=0.26$, $g_{Cl}=6.04$ and $g_{HCO_3}=2.2$. The total conductance across the tissue computed in this way is hence 17.6 mS/cm^2 (or 57 Ω cm^2), which is of the same order of magnitude as the values experimentally measured, which range between 17 and 33 mS/cm^2 (or 30 to 59 Ω cm^2).

Validity of the Fit

In order to ascertain the validity of the computations from which the permeability ratios were derived, those permeability ratios were substituted back into Eq. (1) so that junctional potentials could be calculated and compared with the values experimentally measured. Such comparison is shown in Table 2. As can be seen, the present procedure yields a very reasonable fit.

Discussion

We want to examine the implications of the present results for the different explanations that can be offered for the origin of the potential difference across the endothelial layer. Among other interpretations, we will consider two possibilities: 1) that the PD is due to ionic diffusion across an ion-selective junction subsequent to a solute gradient generated by a neutral pump, or 2) that the PD arises from an electrogenic ion transport mechanism.

As mentioned in the Introduction, both bicarbonate (Hodson & Miller, 1976; Hull et al., 1977) and sodium (Huff & Green, 1981; Lim, 1981*a*, *b*; Lim & Ussing, 1982) net fluxes from stroma to aqueous have been detected across this preparation. Since the net Na^+ movement is in the same direction as that of the HCO_3^- and is similar in magnitude to the particular value of the HCO_3^- flux reported by Hull et al. (1977), the simultaneous presence of such fluxes could be due to a neutral solute transport mechanism. In analogy to an explanation proposed by Machen and Diamond (1969) for the gallbladder, the present polarity observed for the PD could be explained if $NaHCO_3$ would be transported across the cell layer towards the aqueous and then leak back across cation-selective intercellular junctions. As can be seen in Table 2, the present data are consistent with the possibility that the intercellular junctions are slightly more permeant to cations than anions. The permeability sequence is $P_K > P_{Na} > P_{Cl} \cong P_{HCO_3}$.

The low degree of such selectivity (Table 2), however, poses a problem in interpreting the magnitude of the PD measured as a diffusion potential. As can be seen from Figs. 1, 3 and 5, a concentration gradient of about 30 mM of monovalent salt must be imposed in order to obtain a transendothelial PD of about 1 mV. It is unclear whether the endothelium could generate and maintain such a gradient across its leaky junctions. In two other leaky epithelia, the reports vary. Thus, in *Necturus* gallbladder, Curci and Frömter (1979) reported

that the K^+ concentration in the lateral intercellular space is approximately 3.9 mM. This value is significantly higher than that of the K^+ concentration of the bathing solution, which was 2.5 mM, but still the concentration gradient across the junction would be only about 1.4 mM. On the other hand, Gupta, Hall and Naftalin (1978) reported that in rabbit ileum the K^+ concentration in the lateral intercellular space is about 30 mM/kg (of wet weight) and the Na^+ concentration is as high as 160 mM/kg (of wet weight), which are significantly higher than their concentrations in the bathing solution ($[K^+]=15$ mM; $[Na^+]=144$ mM).

In view of the discrepant concentration gradients reported above, it seems useful to examine values that have been predicted for the solute concentration in the intercellular space of the corneal endothelium utilizing theoretical models. The application of the standing gradient osmotic theory (Diamond & Bossert, 1967, 1968) yielded a concentration gradient across the junction of only about 1.5 mM salt (Lim & Fischbarg, 1976). Another calculation based on a somewhat different approach yielded a gradient value of 3 mM (Liebovitch & Weinbaum, 1981). Clearly, such gradients are much lower than the 30 mM that would be required to yield the PD of about 1 mV. In this light, although no concentration gradients have been experimentally measured across this preparation, it appears doubtful that the corneal endothelium could generate and maintain a large concentration gradient across its leaky intercellular junction.

Given the conceptual difficulty in explaining the PD across the endothelium as a diffusion potential across its intercellular junctions, we are left with the second possibility; namely, that such PD arises from electrogenic transport. In this framework, the polarity of the PD could be largely accounted for if the HCO_3^- is electrogenically transported across this preparation. In this connection, Hodson and Miller (1976) found that the activity of carbonic anhydrase in the endothelial cells as gauged by histochemical methods is predominantly localized near the apical (aqueous) cell borders, and implied that such localization could be responsible for electrogenic HCO_3^- transport. However, Lönnerholm (1974) and Lütjen-Drecoll and Lönnerholm (1981) used histochemical techniques also and reported instead that enzyme activity is distributed throughout the cytoplasm. Hence, the basis for a possible mechanism for electrogenic HCO_3^- transport remains unclear.

Turning now to other issues, the resistance measurements given in Figs. 2, 4 and 6 were performed mainly to control that no major adverse effects would be suffered by the tissue due to the different solutions employed. Such seemed to be the case; the transendothelial resistance increase seen upon dilution of the stromal side in Fig. 2 could presumably be attributed to a dilution of the intercellular spaces.

As for the observed effects of osmotic flows on the PD (Figs. 7*a, b*; 8*a, b*), they can be accounted for by "solute polarization" accompanying such flows. In a recent report (Fischbarg & Montoreano, 1982) it is argued that the osmotic permeability of the corneal endothelial cell membranes is very high, which suggests that osmotic flows would take place across the cellular pathway. In consequence, when a sucrose is added to the aqueous side, the water flow from the intercellular spaces into the cells would tend to decrease the volume of the spaces and to leave them hypertonic. Consequently, salt would diffuse through the cation-selective junction into the aqueous and cause a decrease in PD, as seen in see Fig. 7*a*. With the gradient reversed, the PD should increase, and it does so for a short concentration range before it decreases abruptly beyond 20 mOsm/l. However, even if these explanations are qualitatively consistent with the junctional selectivity reported, more complex effects based on secondary changes in the transport mechanism or in the local geometry cannot be excluded.

The authors are grateful to Rona Riegelhaupt, Alan Garten, Ileana Antoniu, Ana Topolovec, and Young K. Kim for their skillful assistance. This work was supported by U.S.P.H.S. Research Grants EY02104 and EY01080.

References

Barfort, P., Maurice, D. 1974. Electrical potential and fluid transport across the corneal endothelium. *Exp. Eye Res.* **19**:11–19

Curci, S., Frömter, E. 1979. Micropuncture of lateral intercellular spaces of *Necturus* gallbladder to determine space fluid K^+ concentration. *Nature (London)* **278**:355–357

Diamond, J.M., Bossert, W.H. 1967. Standing-gradient osmotic flow. A mechanism for coupling of water and solute transport in epithelia. *J. Gen. Physiol.* **50**:2061–2083

Diamond, J.M., Bossert, W.H. 1968. Functional consequences of ultrastructural geometry in "backwards" fluid-transporting epithelia. *J. Cell Biol.* **37**:694–702

Dikstein, D., Maurice, D.M. 1972. The metabolic basis to the fluid pump in the cornea. *J. Physiol. (London)* **221**:29–41

Fischbarg, J. 1972. Potential difference and fluid transport across rabbit endothelium. *Biochim. Biophys. Acta* **228**:362–366

Fischbarg, J. 1973. Active and passive properties of rabbit corneal endothelium. *In: Proc. Intl. Symp. Transp. Eye.* Charleston, S.C., J.A. Zadunaisky, editor. (1972); and *Exp. Eye Res.* **15**:615–638

Fischbarg, J., Lim, J.J. 1973. Determination of the impedance locus of rabbit corneal endothelium. *Biophys. J.* **13**:595–599

Fischbarg, J., Lim, J.J. 1974. Role of cations, anions and carbonic anhydrase in fluid transport across rabbit corneal endothelium. *J. Physiol. (London)* **241**:647–675

Fischbarg, J., Lim, J.J., Bourguet, J. 1977. Adenosine stimulation of fluid transport across rabbit corneal endothelium. *J. Membrane Biol.* **35**:95–112

Fischbarg, J., Montoreano, R. 1982. Osmotic permeabilities across corneal endothelium and antidiuretic hormone-stimulated toad urinary bladder structures. *Biochim. Biophys. Acta* **690**:207–214

Fischbarg, J., Warshavsky, C.R., Lim, J.J. 1977. Pathways for hydraulically and osmotically-induced water flows across epithelia. *Nature (London)* **266**:71–74

Goldman, D.E. 1943. Potential, impedance and rectification in membranes. *J. Gen. Physiol.* **27**:37–60

Gupta, B.L., Hall, T.A., Naftalin, R.J. 1978. Microprobe measurement of Na, K and Cl concentration profiles in epithelial cells and intercellular spaces of rabbit ileum. *Nature (London)* **272**:70–73

Hodgkin, A.L., Katz, B. 1949. The effects of sodium ions on the electrical activity of the great axon of the squid. *J. Physiol. (London)* **108**:37–77

Hodson, S., 1974. The regulation of corneal hydration by a salt pump requiring the presence of sodium and bicarbonate ions. *J. Physiol. (London)* **236**:271–302

Hodson, S., Miller, F. 1976. The bicarbonate ion pump in the endothelium which regulates the hydration of rabbit cornea. *J. Physiol. (London)* **263**:563–577

Huff, J., Green, K. 1981. Effect of temperature and sodium transport inhibition on bicarbonate fluxes in the corneal endothelium. *Curr. Eye Res.* **1**:113–114

Hull, D.S., Green, K., Boyd, M., Wynn, G.R. 1977. Corneal endothelium bicarbonate transport and effect of carbonic anhydrase inhibitors on endothelial permeability and fluxes and corneal thickness. *Invest. Ophthalmol.* **10**:883–892

Klyce, S. 1977. Enhancing fluid secretion by the corneal epithelium. *Invest. Ophthalmol Vis. Sci.* **16**:968–973

Liebovitch, L.S., Weinbaum, S. 1981. A model of epithelial water transport: The corneal endothelium. *Biophys. J.* **35**:315–338

Lim, J.J. 1981*a*. Sodium transport across the rabbit corneal endothelium. *Invest. Ophthalmol Vis. Sci.*, Suppl., p. 195

Lim, J.J. 1981*b*. Na^+ transport across the rabbit corneal endothelium. *Curr. Eye Res.* **1**:255–258

Lim, J.J., Fischbarg, J. 1976. Standing-gradient osmotic flow: Examination of its validity using an analytical method. *Biochim. Biophys. Acta* **443**:339–346

Lim, J.J., Fischbarg, J. 1979. Intra-cellular potential of rabbit corneal endothelial cells. *Exp. Eye Res.* **28**:619–626

Lim, J.J., Fischbarg, J. 1981. Electrical properties of rabbit corneal endothelium as determined from impedance measurements. *Biophys. J.* **36**:677–695

Lim J.J., Ussing, H. 1982. Analysis of presteady-state Na^+ fluxes across the rabbit corneal endothelium. *J. Membrane Biol.* **65**:197–204

Lönnerholm, G. 1974. Carbonic anhydrase in the cornea. *Acta Physiol. Scand.* **90**:143

Lütjen-Drecoll, E., Lönnerholm, G. 1981. Carbonic anhydrase distribution in the rabbit eye by light and electron microscopy. *Invest. Ophthalmol. Vis. Sci.* **21**:782–797

Machen, T.E., Diamond, J.M. 1969. An estimate of the salt concentration in the lateral intercellular spaces of rabbit gallbladder during maximal fluid transport. *J. Membrane Biol.* **1**:194–213

Maurice, D.M. 1969. *In:* The Eye. H. Davson, editor. Academic Press, New York-London

Maurice, D.M. 1972. The location of the fluid pump in the cornea. *J. Physiol. (London)* **221**:43–54

McInnes, D.A. 1939. The Principles of Electrochemistry. Reinhold Publishing Corp, New York

Wiederholt, M., Koch, M. 1978. Intracellular potentials of isolated rabbit and human corneal endothelium. *Exp. Eye Res.* **27**:511–518

Received 18 June 1982; revised 20 September 1982